

University of Arkansas, Fayetteville

ScholarWorks@UARK

Chemical Engineering Undergraduate Honors
Theses

Chemical Engineering

12-2017

Measurement of Peptoid Concentration Using UV Spectroscopy

Katie Holland

Follow this and additional works at: <https://scholarworks.uark.edu/cheguht>



Part of the [Chemical Engineering Commons](#)

Citation

Holland, K. (2017). Measurement of Peptoid Concentration Using UV Spectroscopy. *Chemical Engineering Undergraduate Honors Theses* Retrieved from <https://scholarworks.uark.edu/cheguht/109>

This Thesis is brought to you for free and open access by the Chemical Engineering at ScholarWorks@UARK. It has been accepted for inclusion in Chemical Engineering Undergraduate Honors Theses by an authorized administrator of ScholarWorks@UARK. For more information, please contact scholar@uark.edu.

Abstract

The goal of this research is to establish a relationship between ultraviolet adsorption and peptoid concentration to be used to determine the concentration of an unknown peptoid sample. This will allow for the measurement of concentration differences of peptoid samples before and after incubation with membrane surfaces. Samples were prepared nine know concentrations and diluted 50-fold. The UV absorbances of each sample was measured using a UV spectrophotometer at wavelengths from 200 to 450 nanometers. This process was repeated, and the maximum absorbance of each replicate was averaged to yield an absorbance value for each concentration of peptoid. A linear calibration was obtained, allowing for the prediction of an unknown peptoid concentration. The calibration curve established a linear relationship between peptoid concentration of an original sample diluted 50 times and absorbance with an r-squared value of 0.9595. The application of this curve could replace inaccurate techniques such as weighing solutions.

Table of Contents

Abstract.....	iii
Introduction.....	1
Materials and Methods.....	2
Results and Discussion.....	4
Conclusions.....	7
Acknowledgements.....	8
References.....	9
Appendix A: Graphs and Figures	10
Appendix B: Tables.....	17

Introduction

Biofouling is a widespread problem plaguing membrane applications in many fields. Biofouling includes the accumulation of proteins, microorganisms, cells or other biological molecules on the surface of synthetic membranes when exposed to blood or other biological fluids [1]. Especially in medical applications, the phenomenon of biofouling can prevent membranes from performing their desired function. In many situations biofouling is irreversible; removal of the foulant would cause unacceptable process disruption. In membranes used for applications like an artificial lung, biofouling would decrease the efficiency, membrane lifespan and increase costs [1]. One viable solution to prevent biofouling involves adhering a small layer of polymer layer to membrane surfaces [2].

Biological polymers, including peptoids, consist of a sequence of monomers that dictate both the structure and function of the molecule. Polypeptoids are a classification of synthetic peptidomimetics derived from a N-substituted glycine backbone, whose functionality can be manipulated by slightly altering the backbone structure, in turn changing the chain shape and properties of the polymer [3]. Several factors that tend to increase a surface's propensity to foul include: a charged surface, hydrophobicity, and chemicals that act as hydrogen bond donors or acceptors [4,5]. Structurally, peptoids have no hydrogen bond donors in their flexible backbone, fundamentally contributing to their ability to prevent biofouling [6]. One 5-mer NMEG peptoid (NMEG5) has shown to be effective at preventing fouling up to 66% on an unmodified surface after 2 hours [2].

To increase the ability of NMEG5 to prevent fouling, better methods must be developed to measure how much of the peptoid is being attached membrane surface. With greater attachment the antifouling affects of NMEG5 could potentially increase [2]. Ultraviolet spectrophotometry has been shown to be an effective and fast method of measuring the attachment incurring very few measurement errors in work with single walled nanotubes [7]. The use of UV spectrophotometry to measure peptoid concentration has the potential allow researchers to calculate exactly how much peptoid is being bonded to the surface of membranes, and give more insight into the mechanisms behind the anti-fouling properties of NMEG5.

Materials and Methods

Due to the peptoid having a peak absorbance at approximately 214 nanometers, an ultra violet (UV) spectrophotometer was used to measure the absorbance at wavelengths around this value. Quartz cuvettes, shown in Figure 1, were used to incur minimal disruption at the small wavelengths required to measure the absorbance of the sample. The peak absorbance was utilized to ensure that the maximum sensitivity was captured in the resulting data. This sensitivity ensures that the calibration curve produced will be capable of detecting small peptoid concentration changes in unknown samples.



Figure 1. Quartz Cuvette [8].

The construction of the calibration curve began by considering the absorbance of undiluted versus diluted samples of peptoid at known concentrations. Nine undiluted samples were mixed starting at 4 micromolar and cutting each sample's concentration in half until a concentration of 0.01 micromolar was reached. The second set of samples was comprised of the same concentrations of the first set, but this time the concentration of each sample was diluted 50 times. The diluted set of samples showed the most linear relationship, as discussed in the results section of this report, and was decided to be the best course of action for continuing the research.

The calibration curve was constructed using peptoid concentrated in phosphate buffered saline (PBS) at 0.08, 0.04, 0.02, 0.01, 0.005, 0.0025, 0.00125, 0.000625, and 0.0003125 micromolar. These samples were mixed immediately before the absorbance was measured to ensure no evaporation or peptoid settling in the solvent would alter the results. Each sample set was created by diluting the preceding sample to half of its concentration before the absorbance data was measured. Using the same parent sample ensured that even if the initial sample was not held to the exact labeled concentration, changes in concentrations could still be



Figure 2. UV Spectrophotometer [9].

accurately detected using the calibration curve. Each sample was measured three times, and the maximum absorbance of these three replications was taken as the data point corresponding to each concentration. Running the UV spectrophotometer, similar to the one in Figure 2, three separate times eliminated any measurement error the machine could incur. The process explained above was repeated three times for a freshly mixed parent sample to ensure the accuracy of the calibration curve despite fluctuations in concentration that could have been present in one parent sample.

Results and Discussion

The results from the first undiluted samples are shown in figures 1A-9A in Appendix A. As the samples become more concentrated, noise appears at the peak absorbance. This noise makes it nearly impossible to tell what the peak absorbance is. The maximum points of each concentration of peptoid was taken to produce the curves in Figures 3 and 4 below:

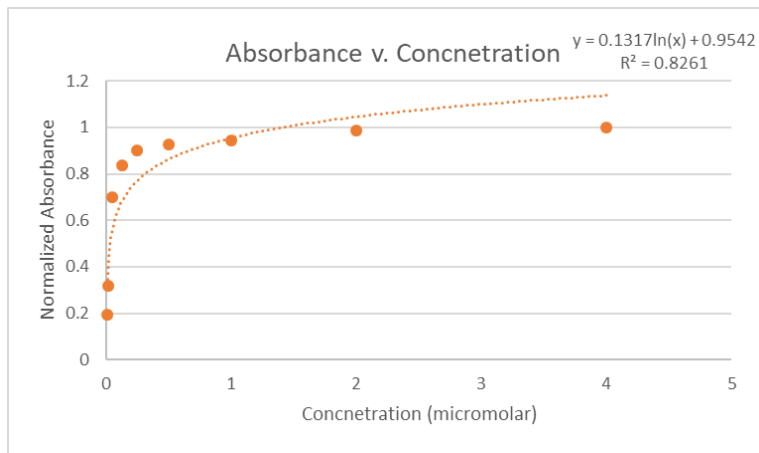


Figure 3. Absorbance versus Peptoid Concentration Undiluted Samples

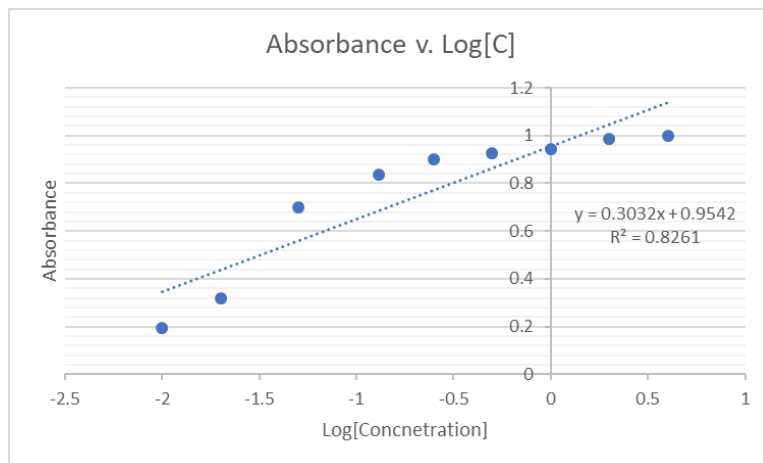


Figure 4. Absorbance versus Log of Peptoid Concentration for Undiluted Samples

The relationship between absorbance and concentration seems to hold has a lose logarithmic, but with an r-squared value of 0.8261 this relationship would not be useful for predicting concentrations of peptoid.

The results of the diluted samples are shown in figures 10A-16A in appendix A. Despite the 0.05 and 0.13 micromolar samples not being concentrated enough to yield desirable results, the diluted samples produced a better relationship between absorbance and concentration as shown in Figure 5 below:

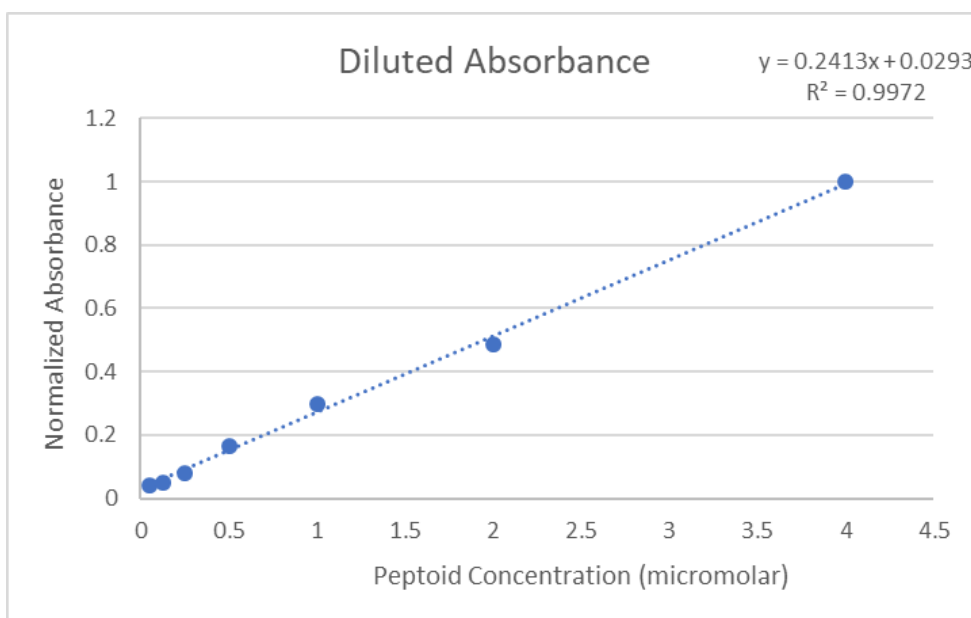


Figure 5. Diluted Absorbance

Once the linear relationship between absorbance and peptoid was established. The process was repeated for three different samples. The results are shown in Appendix B Tables 1B-4B. The resulting relationships from the three trials are included in Appendix A figures 17A-19A. Figure 6 shows the final relationship using the averaged data is shown with the standard error bars included:

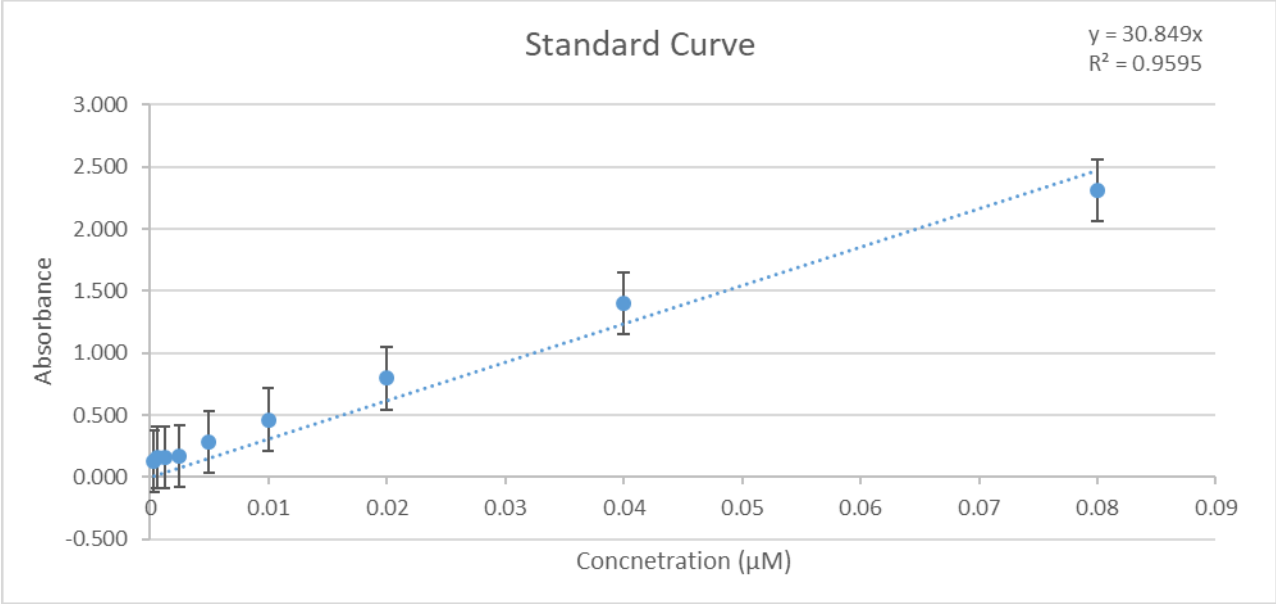


Figure 6: Standard Curve

As can be seen this curve looks very similar to figure 6. The repetitions eliminate error that could have been present in the initial trial.

Conclusion

The strong linear relationship ($r\text{-squared} = 0.9595$) between absorbance and concentration of peptoid indicates using UV absorbance as a method of measuring peptoid concentrations will be effective in research. Using this relationship will allow researchers to abandon other tedious and inaccurate procedures used to account for peptoid being attached to membrane surfaces. One concern with the relationship is the relatively large standard deviations associated with each data point. For measuring larger concentration differences, the curve is useful, but if the concentration difference being measured is very small further trials are recommended.

Acknowledgements

I would like to thank Dr. Servoss and Neda Mahmoudi for allowing me the opportunity to work on this research and instructing me along the way. I would like to thank Dr. Beitle for allowing us to use his UV Spectrophotometer and making room for our research in his lab. I would also like to thank the University of Arkansas Department of Chemical Engineering for supporting me as I am working to attain my Bachelor's of Science in Chemical Engineering with Honors.

References

1. Ham, Hyun Ok, Sung Hyun Park, Josh W. Kurutz, Igal G. Szleifer, and Phillip B. Messersmith. 2013. Antifouling glycoalkalix-mimetic peptoids. *Journal of the American Chemical Society* 135 (35): 13015.
2. Mahmoudi, N., Reed, L., Moix, A., Alshammari, N., Hestekin, J., Servoss, S. (2016). PEG-Mimetic Peptoid Reduces Protein Fouling of Polysulfone Hollow Fibers. *Colloids and Surfaces B: Biointerfaces*. 149. 10.1016/j.colsurfb.2016.09.038.
3. van Zoelen, W., Zuckermann, R. N., Segalman, R. A. Tunable Surface Properties from Sequence-Specific Polypeptoid–Polystyrene Block Copolymer Thin Films *Macromolecules*. 2012, 45, 7072– 7082, DOI: 10.1021/ma3009806
4. Jeffrey L. Dalsin, Phillip B. Messersmith, Bioinspired antifouling polymers, In *Materials Today*, Volume 8, Issue 9, 2005, Pages 38-46, ISSN 1369-7021
5. Holmlin, R., Xiaoxi Chen, R., Chapman, S., Whitesides, G., Zwitterionic, SAMs that Resist Nonspecific Adsorption of Protein from Aqueous Buffer *Langmuir*, 2001, 17 (9), 2841-2850, DOI: 10.1021/la0015258
6. Kirshenbaum, Kent, B., Goldsmith, R., Armand, P., Bradley, E., Truong, K., Dill, K., Cohen, F., Zuckermann, R., "Sequence-specific polypeptoids: A diverse family of heteropolymers with stable secondary structure." 1998. *Proceedings of the National Academy of Sciences* 95 (8):4303-4308.
7. Attal, S.; Thiruvengadathan, R.; Regev, O. Determination of the Concentration of Single-Walled Carbon Nanotubes in Aqueous Dispersions Using UV–Visible Absorption Spectroscopy. *Analytical Chemistry* 2006 78 (23), 8098-8104. DOI: 10.1021/ac060990s
8. "Cuvettes." Cole-Parmer, Cole-Parmer, www.coleparmer.com/c/cuvettes.
9. "BECKMAN DU 530 SPECTROPHOTOMETER." Beckman DU 530 Spectrophotometer, www.thelabworldgroup.com/beckman-DU-530-spectrophotometer.

Appendix A:

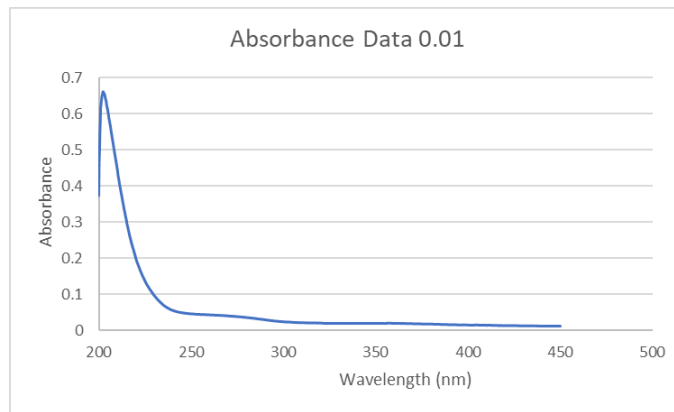


Figure 1A: Undiluted 0.01 Micromolar

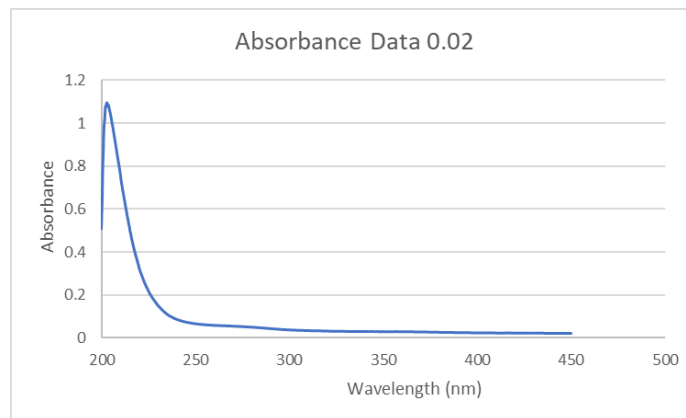


Figure 2A: Undiluted 0.02 Micromolar

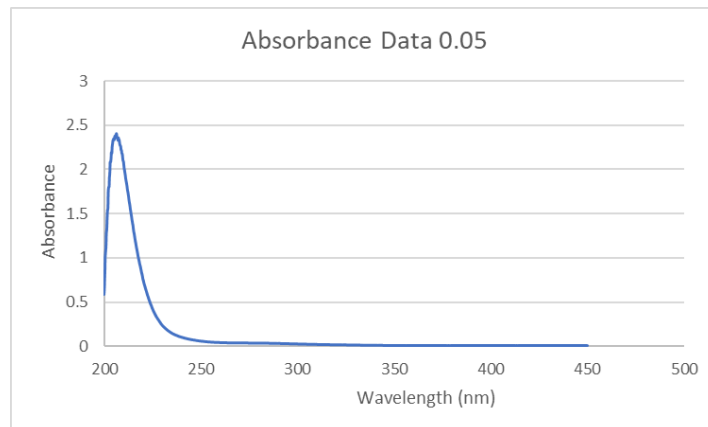


Figure 3A: Undiluted 0.05 Micromolar

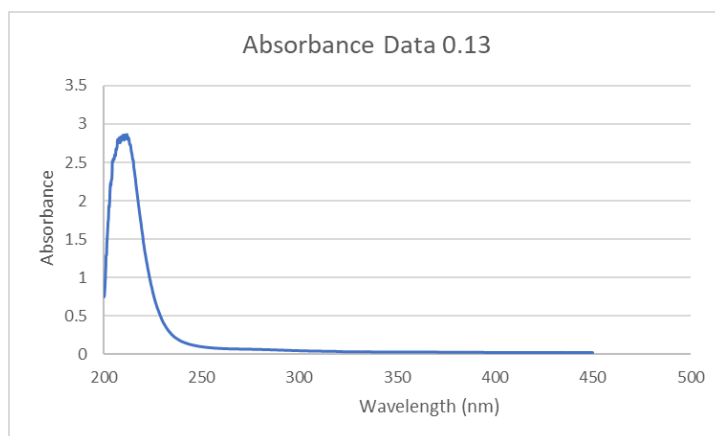


Figure 4A: Undiluted 0.13 Micromolar

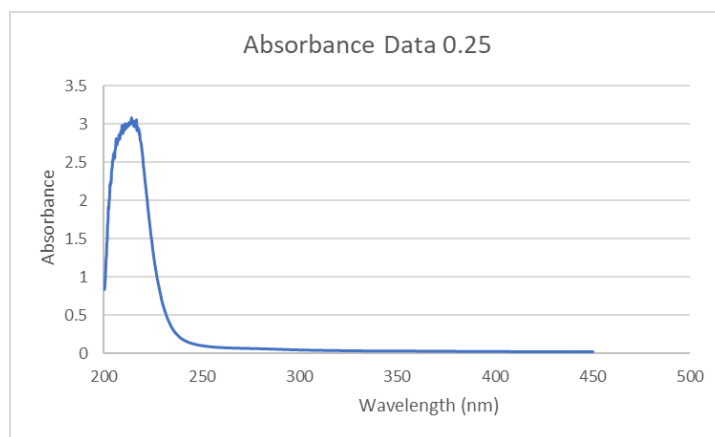


Figure 5A: Undiluted 0.25 Micromolar

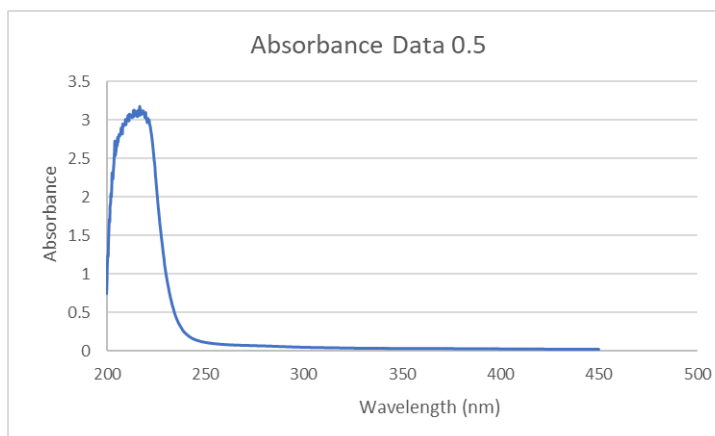


Figure 6A: Undiluted 0.5 Micromolar

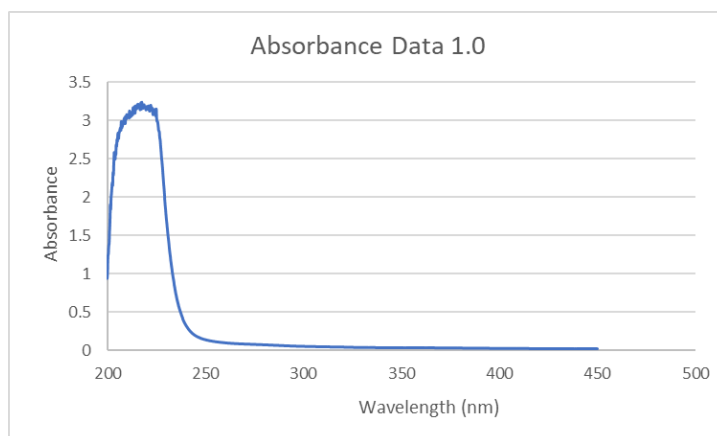


Figure 7A: Undiluted 1.0 Micromolar

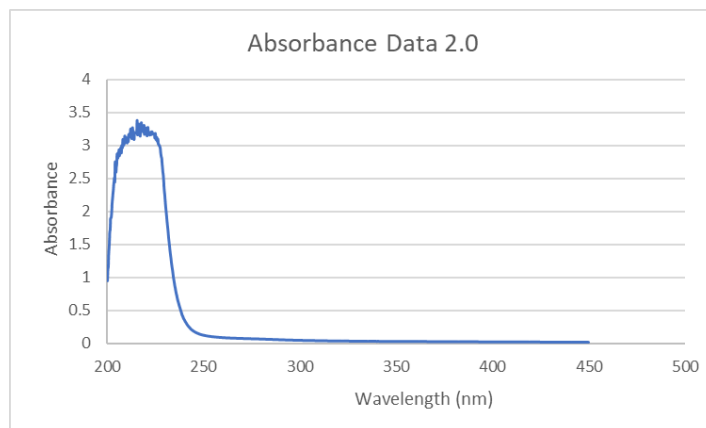


Figure 8A: Undiluted 2.0 Micromolar

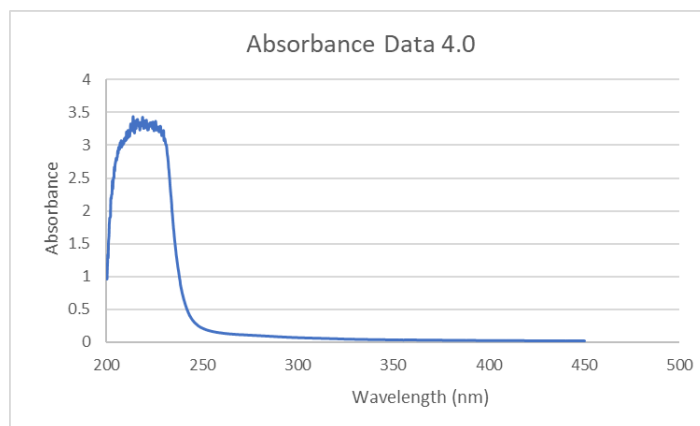


Figure 9A: Undiluted 4.0 Micromolar

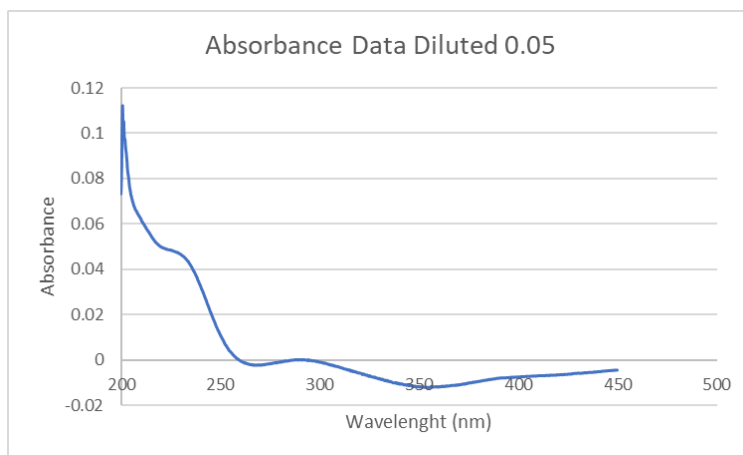


Figure 10A: Diluted 50x 0.05 Micromolar

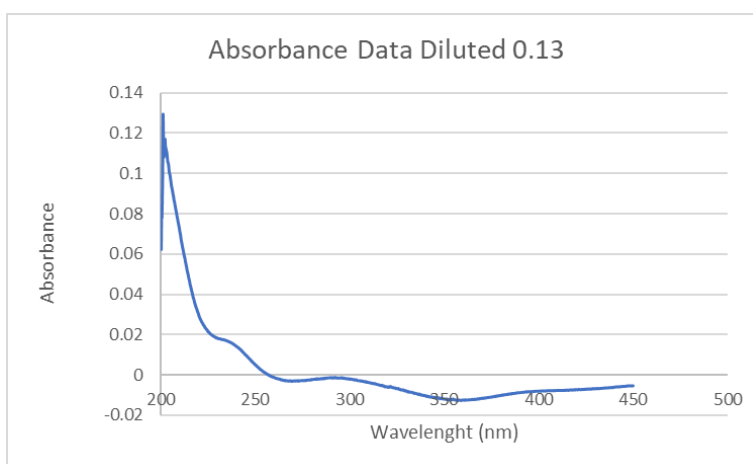


Figure 11A: Diluted 50x 0.13 Micromolar

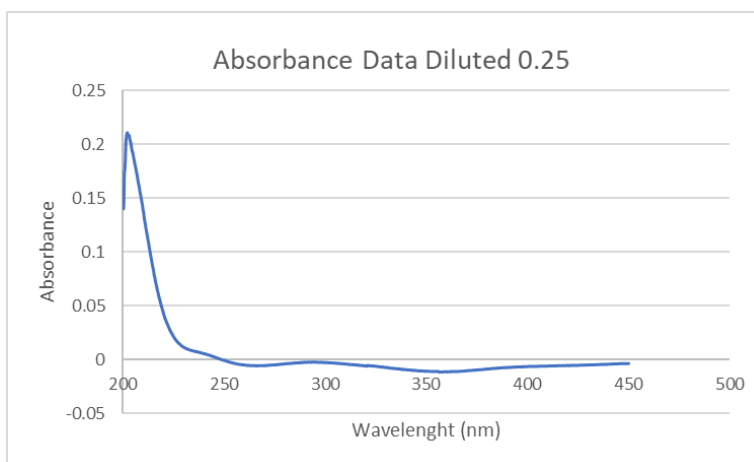


Figure 12A: Diluted 50x 0.25 Micromolar

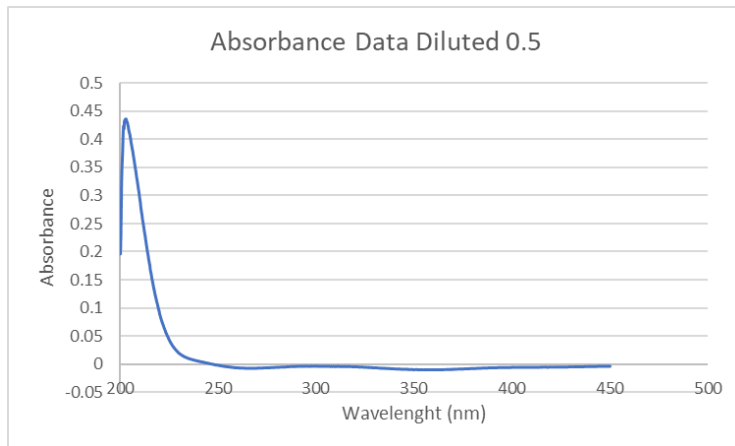


Figure 13A: Diluted 50x 0.5 Micromolar

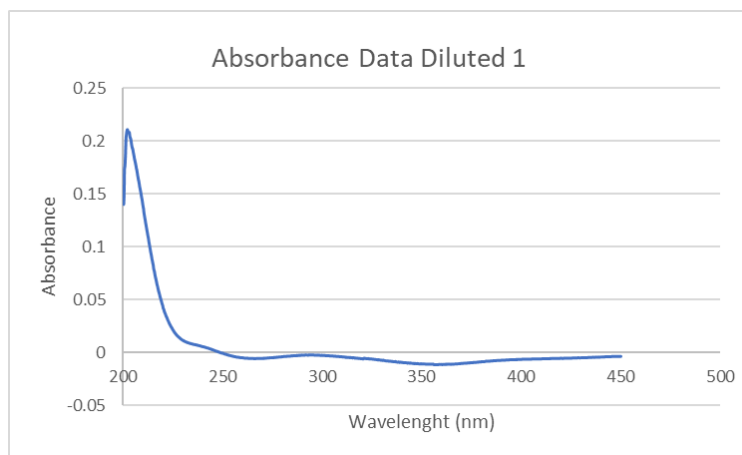


Figure 14A: Diluted 50x 1.0 Micromolar

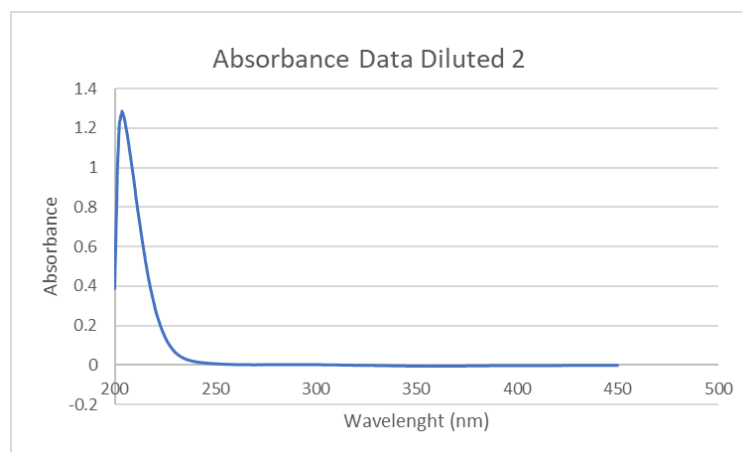


Figure 15A: Diluted 50x 2.0 Micromolar

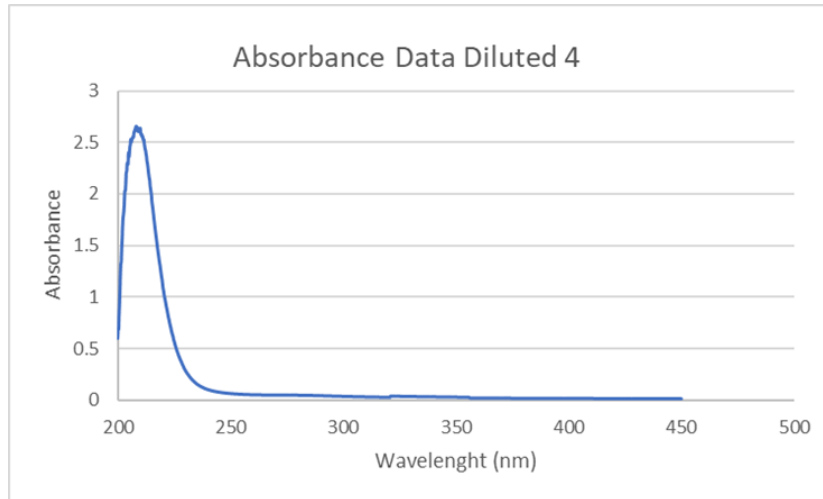


Figure 16A: Diluted 50x 4.0 Micromolar

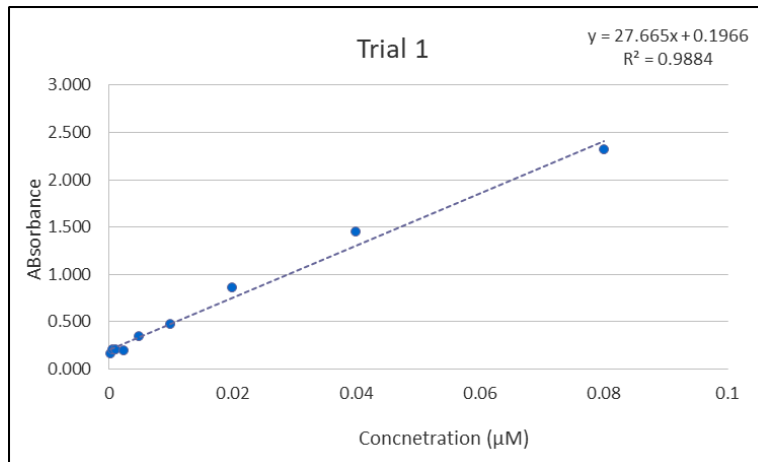


Figure 17A: Calibration Curve Trial 1

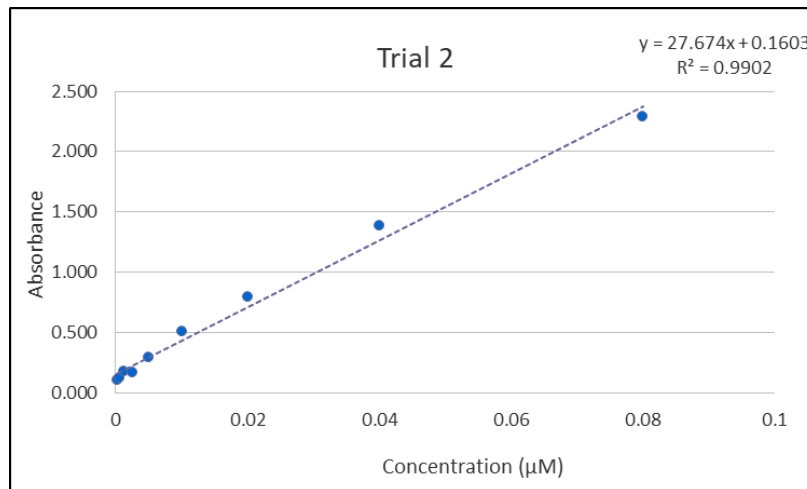


Figure 18A: Calibration Curve Trial 2

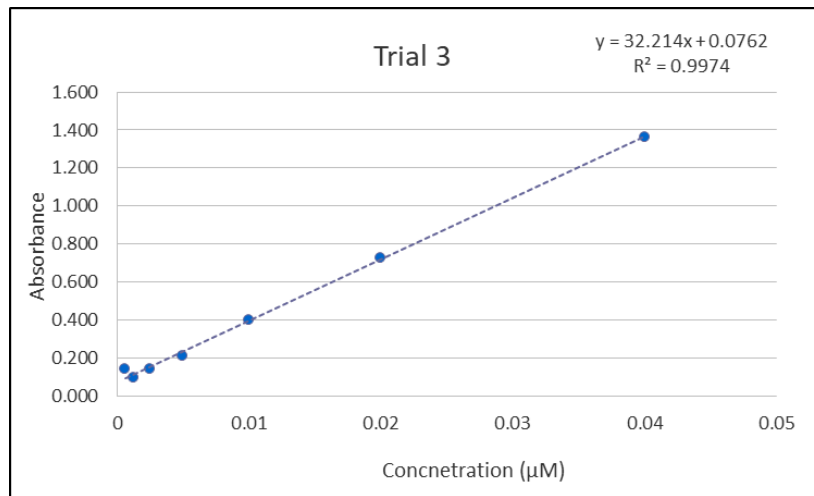


Figure 19A: Calibration Curve Trial 3

Appendix B

Table 1B: Trial 1 Results

Trial 1	Max Absorbance			
Concentration (μM)	Replication 1	Replication 2	Replication 3	Average
0.0003125	0.127	0.162	0.181	0.156
0.000625	0.162	0.208	0.234	0.201
0.00125	0.174	0.202	0.222	0.199
0.0025	0.180	0.201	0.211	0.197
0.005	0.325	0.340	0.349	0.338
0.01	0.461	0.473	0.486	0.473
0.02	0.848	0.858	0.875	0.860
0.04	1.446	1.450	1.450	1.449
0.08	2.305	2.320	2.312	2.312

Table 2B: Trial 2 Results

Trial 2	Max Absorbance			
Concentration (μM)	Replication 1	Replication 2	Replication 3	Average
0.0003125	0.096	0.105	0.114	0.105
0.000625	0.119	0.127	0.135	0.127
0.00125	0.170	0.179	0.185	0.178
0.0025	0.164	0.176	0.184	0.175
0.005	0.265	0.302	0.324	0.297
0.01	0.491	0.517	0.525	0.511
0.02	0.784	0.801	0.806	0.797
0.04	1.374	1.382	1.394	1.383
0.08	2.298	2.275	2.294	2.289

Table 3B: Trial 3 Results

Trial 3		Max Absorbance			
Concentration (μM)	Replication 1	Replication2	Replication3	Average	
0.000625	0.138	0.128	0.142	0.142	
0.00125	0.067	0.067	0.098	0.098	
0.0025	0.138	0.128	0.142	0.142	
0.005	0.216	0.208	0.213	0.213	
0.01	0.400	0.401	0.404	0.404	
0.02	0.728	0.726	0.728	0.728	
0.04	1.368	1.372	1.364	1.364	
0.08	2.321	2.321	2.321	2.321	

Table 4B: Overall Results

Overall Results		Max Absorbance			
Concentration (μM)	Replication 1	Replication 2	Replication 3	Average	Standard Deviation
0.0003125		0.105	0.156	0.131	0.026
0.000625	0.142	0.127	0.201	0.157	0.032
0.00125	0.098	0.178	0.199	0.158	0.044
0.0025	0.142	0.175	0.197	0.171	0.023
0.005	0.213	0.297	0.338	0.283	0.052
0.01	0.404	0.511	0.473	0.463	0.044
0.02	0.728	0.797	0.860	0.795	0.054
0.04	1.364	1.383	1.449	1.399	0.037
0.08	2.321	2.289	2.312	2.307	0.014